

# Analysis of Cut-off Conditions for Coaxial Fibers

Humberto Filomeno da Silva

*Departamento de Física, Centro de Ciências Exatas e Tecnologia  
Universidade Federal do Maranhão, Av. dos Portugueses, S/N  
Campus do Bacanga, Sao Luís, MA, Brazil - CEP 65080-042*

and Frederico Dias Nunes

*Departamento de Eletrônica e Sistemas, Centro de Tecnologia  
Universidade Federal de Pernambuco  
Caixa Postal 7800, 50711-970, Recife, PE, Brazil*

Received on 21 June, 2000. Revised version received on 20 September, 2000

This paper reports the analysis of modal normalized frequency cut-off of coaxial fibers having four dielectric layers. The cut-off curves are obtained for four different structures and several modes as a function of the several parameters of the fibers (refractive index and layer dimension). The calculation is done using a transcendental equation obtained in this work. The analysis pays a special attention to the fundamental mode  $HE_{11}$  showing that for two structures (W1 and M1) the normalized frequency always is null as is the case of the standard rod fibers. For the other two structures (W2 and two regions), the normalized frequency may not be null, depending on the set of values of the fiber parameters. For this last case a loci diagram is obtained showing the regions where the normalized frequency is equal to zero and different from zero for several sets of fiber parameters. From the transcendental equation, we have an expression to calculate the curve of separation between these two regions.

## I Introduction

Cozens and Boucouvalas [1] introduced a new structure of optical fibers having four dielectric layers with which it has been possible to develop different devices such us sensors and spectral filters [2]. Nunes et al [3] have published, for the first time, a detailed theoretical study of four different structures of coaxial fibers. The transcendental equations for each structure were obtained for all the ranges of physically acceptable values of the effective refractive index. This work brings complementary results to those of Ref. [3], being focused on the analysis of the cut-off behavior of the structures W and M [3]. Their refractive index profiles are shown in Fig. 1 and, as indicated, both structures W and M have been sub-classified as 1 and 2.

The structure W1 and been used to manufacture spectral filters [2] with promising characteristics for optical communications and dispersion compensating fiber [4] with large negative dispersion coefficient  $D$  for the fundamental mode. For example, the filters are made with fiber tapers and its physical behavior is mainly described using perturbative theory, local mode (LM) approximation [5], taking into account the modes

$HE_{11}$  and  $HE_{12}$ . With the LM approach it is seen that the coupling between  $HE_{11}$  and  $HE_{12}$  is a fundamental part on the device description. However, coupling will only occur if both modes exist. If one of them is under the cut-off condition, no coupling can occur and the device is unable to operate showing the necessity of understanding the cut-off conditions.

The cut-off condition for one mode is dependent on the fiber parameters and light wavelength. In the specific case of W coaxial fibers with four dielectric layers, there are seven parameters to be considered: four values of refractive index and three dimensions (Fig. 1). These parameters are reduced to four according to which the cut-off conditions are analyzed. The values  $V$  of cut-off normalized frequency are calculated solving a transcendental equation that we have obtained and is given in section III. The results show that in the case of the structure W2 and M2 the fundamental mode has a non vanishing  $V$ , contrary to the structure W1 and M1 for which  $V$  always vanishes as is the case of common core-clad fibers [6].

## II Mathematical approach

The propagation characteristic of a coaxial fiber can be described using the well-known LP approximation. This is the approach that we use in this work and in this section we present a brief discussion of the results widely detailed in Ref. [3]. The modal wavefunctions will be those given by

$$\psi(\rho, \theta, z) = \varphi(\rho, \theta) \exp(i\beta z) \quad (1)$$

where  $\psi$  may be  $E_y$  or  $E_x$ , depending on the choice between the two possible linearly polarized LP solutions [3],  $z$  is the direction of propagation and  $\beta$  is the propagation constant. In eq. (1),  $\varphi(\rho, \theta)$  is given by:

$$\varphi(\rho, \theta) = R(\rho) \left\{ \begin{array}{l} \cos(m\theta) \\ \sin(m\theta) \end{array} \right\}, \quad m = 0, 1, 2, \dots \quad (2)$$

where  $\theta$  is the azimuth angle and  $m$  is the parameter that defines the azimuth LP mode order. The solution in sine or cosine follows from the choice of polarization [3].  $R(\rho)$  is the transverse solution given as a combination of the well known Bessel and Modified Bessel functions of first and second classes. In each region, an appropriate combination of Bessel functions is required to match the conditions of convergence that is

dependent on the range of the modal effective refractive index. With this approach, transcendental equations [3] are obtained for each structure and they describe the fibers completely. For the structures W1 and M1 the transcendental equation is that corresponding to  $N_e$  (effective refractive index) within the range  $(n_2, n_4)$  [3]. For the structures W2 and M2 the transcendental equation is that corresponding to  $N_e$  within the range  $(n_1, n_4)$  [3].

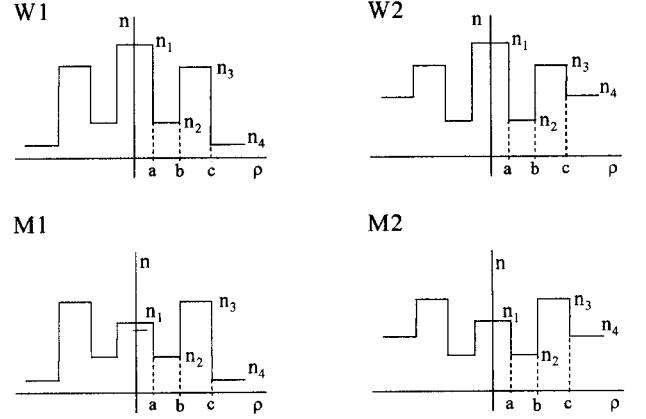


Figure 1. Coaxial optical fibers profiles for the structures W1, W2, M1 and M2.

Table 1 - Parameters of eq.(3)

W1 and M1	W2 and M2
$A = W_3 Y_{\ell+1}(W_3) Y_{\ell}(U_3) - U_3 Y_{\ell+1}(U_3) Y_{\ell}(W_3)$	$A = W_3 K_{\ell+1}(W_3) Y_{\ell}(U_3) - U_3 Y_{\ell+1}(U_3) K_{\ell}(W_3)$
$B = W_2 Y_{\ell+1}(W_2) J_{\ell}(U_1) - U_1 J_{\ell+1}(U_1) Y_{\ell}(W_2)$	$B = U_1 J_{\ell+1}(U_1) K_{\ell}(W_2) - W_2 K_{\ell+1}(W_2) J_{\ell}(U_1)$
$C = W_3 J_{\ell+1}(W_3) Y_{\ell}(U_3) - U_3 Y_{\ell+1}(U_3) J_{\ell}(W_3)$	$C = W_3 I_{\ell+1}(W_3) Y_{\ell}(U_3) + U_3 Y_{\ell+1}(U_3) I_{\ell}(W_3)$
$D = W_2 J_{\ell+1}(W_2) J_{\ell}(U_1) - U_1 J_{\ell+1}(U_1) J_{\ell}(W_2)$	$D = W_2 I_{\ell+1}(W_2) J_{\ell}(U_1) + U_1 J_{\ell+1}(U_1) I_{\ell}(W_2)$
$E_1 = W_3 Y_{\ell+1}(W_3) J_{\ell}(U_3) - U_3 J_{\ell+1}(U_3) Y_{\ell}(W_3)$	$E_1 = W_3 K_{\ell+1}(W_3) J_{\ell}(U_3) - U_3 J_{\ell+1}(U_3) K_{\ell}(W_3)$
$E_2 = W_3 J_{\ell+1}(W_3) J_{\ell}(U_3) - U_3 J_{\ell+1}(U_3) J_{\ell}(W_3)$	$E_2 = W_3 I_{\ell+1}(W_3) J_{\ell}(U_3) + U_3 J_{\ell+1}(U_3) I_{\ell}(W_3)$

## III Cut-off condition

The cut-off condition for any mode of the coaxial fiber that we are analysing occurs when its effective refractive index  $N_e$  equals to  $n_4$ . Following this, the cut-off condition for all fibers can be imposing making  $N_e = n_4$  in the arguments of the Bessel function of the corresponding transcendental equations. By doing so, some problems occur because the modified Bessel function  $K_m(W_4)$  diverges for very small values of  $W_4$ . These problems can be overcome using the small argument approximation for the Bessel functions [7]. With this

approximation in the transcendental equation for the effective refractive index and easy mathematical manipulations, the cut-off frequency can be calculated by solving the following transcendental equation:

$$\left[ \frac{2\ell J_{\ell}(U_4) - U_4 J_{\ell+1}(U_4)}{2\ell J_{\ell}(U_4) - U_4 Y_{\ell+1}(U_4)} \right] (AD \mp BC) = (E_1 D \pm E_2 B), \quad \ell = 0, 1, 2, \dots \quad (3)$$

where  $U_4$ ,  $A$ ,  $B$ ,  $C$ ,  $D$ ,  $E_1$  and  $E_2$  are parameters given in the Tables 1, 2 and 3. In Table 2,  $A$  and  $R$  are defined as:  $A = \frac{a}{c}$ ,  $R = -\frac{b-a}{c}$  (Fig. 1). The minus sign found in both sides of eq. (3) is applied for both struc-

tures W1 and M1 while the plus sign to the structures W2 and M2. The numeric solutions of the eq. (3) for

$V_i$  ( $i=1,2,3,4$ ) are shown and discussed in the section IV.

Table 2 - Bessel function's arguments where  $V_1 = ck_0(n_1^2 - n_3^2)^{1/2}$ ,  $V_2 = ck_0(n_3^2 - n_4^2)^{1/2}$ ,  $V_3 = V_1$  and  $V_4 = ck_0(n_3^2 - n_2^2)^{1/2}$ .

W1	W2	M1	M2
$U_1 = \frac{V_1 A}{(1 - q_1^2)^{1/2}}$	$U_1 = V_3 \left( \frac{1 - p_2^2}{1 - q_2^2} \right)^{1/2} A$	$U_1 = V_2 A q_3$	$U_1 = V_4 (q_4^2 - p_4^2)^{1/2} A$
$U_3 = \frac{V_1 q_1 (R + A)}{(1 - q_1^2)^{1/2}}$	$U_3 = V_3 \left( \frac{q_2^2 - p_2^2}{1 - q_2^2} \right)^{1/2} (R + A)$	$U_3 = V_2 (R + A)$	$U_3 = V_4 (1 - p_4^2)^{1/2} (A + R)$
$U_4 = \frac{V_1 q_1}{(1 - q_1^2)^{1/2}}$	$U_3 = V_3 \left( \frac{q_2^2 - p_2^2}{1 - q_2^2} \right)^{1/2}$	$U_4 = V_2$	$U_4 = V_4 (1 - p_4^2)^{1/2}$
$W_2 = \frac{V_1 p_1 A}{(1 - q_1^2)^{1/2}}$	$W_2 = \frac{V_3 p_2 A}{(1 - q_2^2)^{1/2}}$	$W_2 = V_2 p_3 A$	$W_2 = V_4 p_4 A$
$W_3 = \frac{V_1 p_1 (R + A)}{(1 - q_1^2)^{1/2}}$	$W_3 = \frac{V_3 p_2 (R + A)}{(1 - q_2^2)^{1/2}}$	$W_3 = V_2 p_3 (R + A)$	$W_3 = V_4 p_4 (A + R)$

A special attention is given to the mode HE<sub>11</sub> because it is the most common excited mode of the fiber in practical applications. As we will show in the next section, eq. (3) just admits solution for discret values of  $V_i$  ( $i=1,2,3,4$ ) for a certain value of  $\ell$ . Then, the study of eq. (3) assuming  $\ell = 0$  and close to  $V_i = 0$ , allows to determine when the fundamental mode presents a cut-off different from zero.

For this purpose, we will define the function  $G$  as the difference between the right and left sides of eq. (3). Following the analysis of Safaai-Jazi et al [6,8], we will use the condition  $\ell = 0$  and  $V_i \rightarrow 0$  in  $G$ . In the limit where  $V_i$  is small, all Bessel functions present expansions [7] for small arguments.

Substituting these expansions in  $G$ , making the necessary manipulations and maintaining the terms of linear order in  $V$  we obtains:

$$G = f_i V_i, \quad \text{for } i = 1, 2, 3, 4 \quad (4)$$

where  $f_i$  is a function that depend on the parameters and kind of the coaxial fiber under analysis, and are show in Table 4.  $G$  in eq. (4) shows a linear depen-

dence when  $V_i$  is close to zero. When  $V_i$  tends to 0,  $G$  should tend to zero for  $V_i$  to be a solution of eq. (3). For the fibers W1 and M1,  $f_i$  ( $i=1,2$ ) in eq. (4) is always positive and different from zero for any values of the fibers parameters. For  $G$  to be null in this limit we must always have  $V_i = 0$ . In these cases the fundamental mode has a null cut-off.

The situation is different for fibers W2 and M2. In the limit  $V_i \rightarrow 0$  ( $i=3,4$ ),  $G$  can be zero using the condition  $f_i = 0$  for these fibers. In this case  $V_i$  can be different from zero. This condition allows to determine the relationship between the parameters of the fiber starting from where  $V_i$  become different from zero.

## IV Results

We first present the results of an important case corresponding to the cut-off normalized frequency of the fundamental mode. As is well known in conventional core-clad fibers, the mode HE<sub>11</sub> always has a cut-off equal to zero [6]. As it was shown, this fact occurs in the case of the structures W1 and M1.

For the structures W2 and M2,  $f_i$  ( $i=3,4$ ) may change its signal depending on the set of values of the fibers parameters. Then  $f_i = 0$  is the limit condition for  $G = 0$  in eq. (4) with  $V_i \neq 0$  ( $i=3,4$ ). Therefore, depending on the values of the dimensional parameters and of the refractive indexes, the fundamental mode has  $V_i = 0$  or  $V_i \neq 0$ . This behavior is already found in three layers fibers as reported by Safaai-Jazi [6] and Mahmaud et al [9].

The limit equations obtained in this work for the structures W2 and M2 can be checked-up in the case some limit structures. For example, making  $a = 0$  ( $A = 0$ ), the coaxial fiber W2 is reduced to the structure studied by Mahmaud et al [9], as shown in Fig 2.a. The critical value  $b/c$  is obtained in this work making  $A = 0$  in the equation  $f_3 = 0$  for the W2 structure given in the Table (4):

$$\frac{b}{c} = \left( \frac{n_3^2 - n_4^2}{n_3^2 - n_2^2} \right)^{1/2} \quad (5)$$

This result reproduces that of Ref. [9]. Mahmaud et al show that for  $b/c$  larger than the value supplied by the eq. (5), the fundamental mode present cut-off different from zero.

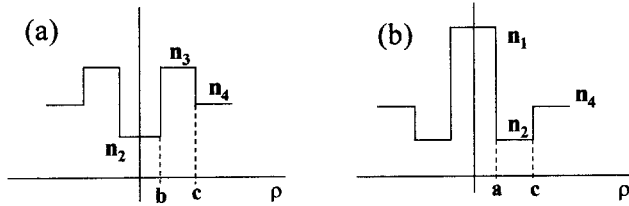


Figure 2. Limit structures for the fiber W2.

By making  $b = c$  ( $R = 0$ ) in the equation  $f_3 = 0$  for the W2 structure, we reproduced the results of the structure studied by Adams [10], shown in Fig. 2.b. The critical value  $a/c$  obtained in this work is:

$$\frac{a}{c} = p_2 = \left( \frac{n_4^2 - n_2^2}{n_1^2 - n_2^2} \right)^{1/2} \quad (6)$$

that is in agreement with Ref. [10]. We will analyze  $V_i$  ( $i=1,2,3,4$ ) for different modes as function of the other parameters of the fiber. This analysis will be made through numerical solution of eq. (3) for the referred structure. In order to avoid exceeding number of figures, we have chosen a few convenient modes and  $V_i$  is studied as a function of the parameter  $R$  for different sets of the remaining parameters.

## IV.1 W1 structure

Fig. 3(a,b) show  $V_1$  as a function of  $R$  for different modes  $\text{HE}_{11}$  ( $n=2,3$ ) and  $\text{HE}_{21}$  for the structure W1. As it is well known, the mode  $\text{HE}_{21}$  is the higher order mode next to  $\text{HE}_{11}$  permitted to propagate in standard fibers [8]. The parameter  $R$  in this figure has values in the range  $[0,1-A]$ . In the extreme values of the  $R$  the W1 structure is reduced to a three region double clad structure.

The W1 structure always has a vanishing cut-off frequency for the fundamental mode according to arguments presented after the deduction of eq. (4). For other modes,  $V_1$  has non-vanishing values which increase for increasing  $R$  and order modes, presenting quasi-oscillatory behavior. These oscillations were also reported by Boucouvalas et al [11] for a coaxial fiber with  $n_1 = n_3$  and  $n_2 = n_4$ . Because the coaxial fiber has many parameters it is not easy to separate their specific influence on the  $V$ , behavior shown in Fig. 3(a,b). In order to explain the oscillations we suggest that this behavior is caused by the competition between the two coupled substructures that compose the coaxial fiber. As discussed in Ref. [11], the coaxial fiber is a structure formed by two coupled structures, namely rod and tube. For small  $R$  values, the rod characteristic tends to be dominant due to its stronger confinement character compared to the tube structure. On the other hand, in the range where the tube characteristic is dominant (large  $R$  values),  $V$ , increases faster. For  $R$  between these extreme values it is not clear who dominates the competition. In this interval of  $R$ ,  $V_1$  present an intermediary behavior between the two limiting situations. Fig. 4 shows the behavior of the confinement factors (between the energy contained in certain layer of refractive index and the total energy), very close to the cut-off conditions for the modes  $\text{HE}_{12}$  and  $\text{HE}_{13}$ . In these graphs,  $g_1$  is the confinement factor of the core,  $g_2$  is the confinement factor of the region of the refractive index  $n_2$ ,  $g_3$  is the confinement factor of the region of the refractive index  $n_3$ ,  $F = 1 - (g_1 + g_2 + g_3)$  and cut-off is the normalized cut-off curve. These graphs show that, if the cut-off curve is approximately constant, all fractions of energy contained in each layer are approximately constant. We point out that the  $V_1$ , curves corresponding to modes  $\text{HE}_{21}$  and  $\text{HE}_{12}$  have a crossing point, as observed in Fig. 3b. This is also observed in the structure analyzed by Boucouvalas et al [10] and indicates that for some sets of fiber parameters, the mode  $\text{HE}_{21}$ , is no longer the lowest mode subsequent to the mode  $\text{HE}_{11}$ , but the mode  $\text{HE}_{12}$ .

Fig. 3a shows that small values of  $p_1$  take the largest values of  $V_1$  for  $R > 0.1$ . It is easy to see that lower values of  $p_1$ , with constant  $q_1$ , correspond to lower values of  $n_2$  resulting in a large step ( $n_1 - n_2$ ) in the gap region and as a consequence, weaker confinement that leads to higher values of  $V_1$ . For  $R < 0.1$ , the cut-off frequency does not change for different values of  $p_1$  because practically does not exist a region in the fiber corresponding to the refractive index  $n_2$ . Thus, there is no significant change on  $V_1$  when  $p_1$  is modified. The same behavior occurs in Fig. 4b, but in this case,  $V_1$  is smaller in the whole range of  $R$  because the extension of the nucleus is larger, increasing the confinement of the modes.

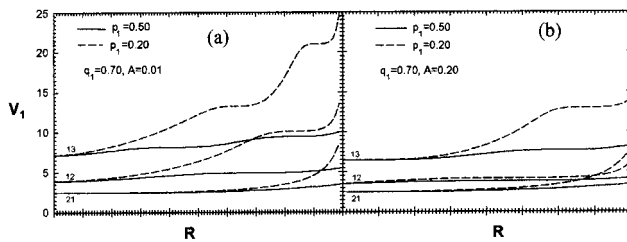


Figure 3. Coaxial fiber cut-off frequencies for the modes 12, 13 and 21 for different values of  $q_1$  and  $p_1$  in the W1 structure.

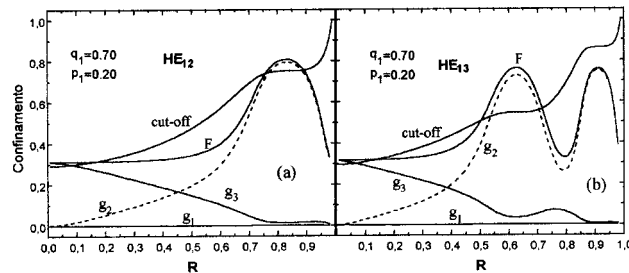


Figure 4. Confinement factor for the W1 structure next to the cut-off with  $A=0.01$ . The cut-off curve is the normalized cut-off curve. (a)  $HE_{12}$  mode. (b)  $HE_{13}$  mode.

The analyses carried out to understand the variation of  $p_1$  and  $q_1$  can be summarized with the following rule: *the modal confinement increases in the proximity of the cut-off condition ( $V_1$  decreases) if the refractive indices satisfy the following condition  $n_1 \cong n_2 \cong n_3$ .* Applying this rule to analyze the graphs of the structure W1 allows us to understand the trends of the curves.

## IV.2. M1 Structure

The M1 structure has a behavior similar to that of the W1 structure and the same kind of analyses can be done for this structure. It is a remarkable fact that the rule valid to describe the behavior of  $V_1$  for the W1 structure is also valid to describe the behavior of  $V_2$  for the M1 structure. A comment is that, for a small rod dimension,  $V_2$  is basically independent of the parameter  $q_3$ . This occurs when  $A$  is very small and because  $n_1 < n_3$ . Then, the influence of the rod region on the fiber characteristic is almost known.

## IV.3. W2 structure

The cut-off values of  $V_3$  for the structure W2 is presented in Fig. 5 (a,b). This structure presents very different behavior in comparison with those of the structures W1 and M1. The structure is free of oscillations, presenting a strong dependence on  $R$  when this parameter approaches the limiting values  $R = 1 - A$ . This behavior indicates that a reduced competition between the two substructures occurs and the tube substructure is dominant in almost all range of  $R$ . Also, no crossing point is observed between the  $V_3$  curves of different modes as is the case of the W1 and M1 fibers. The sharp dependence of the cut-off normalized frequency for the structure W2 on  $R$  indicates a weak modal confinement that is associated with the high refractive index of the clad region ( $n_4 > n_2$ ). Another great difference studied refers to the behavior of the fundamental mode. For this mode, a critical value of  $R$  exists above which  $V_3$  is different from zero. This critical value depends on the set of the fiber parameters being found, imposing that  $f_3$  in the Table 4 is null. Then,

$$= \left( 1 + \frac{A^2 - p_2^2}{q_2^2} \right)^{1/2} - A \quad (7)$$

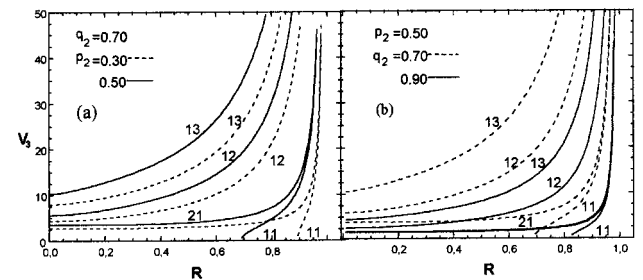


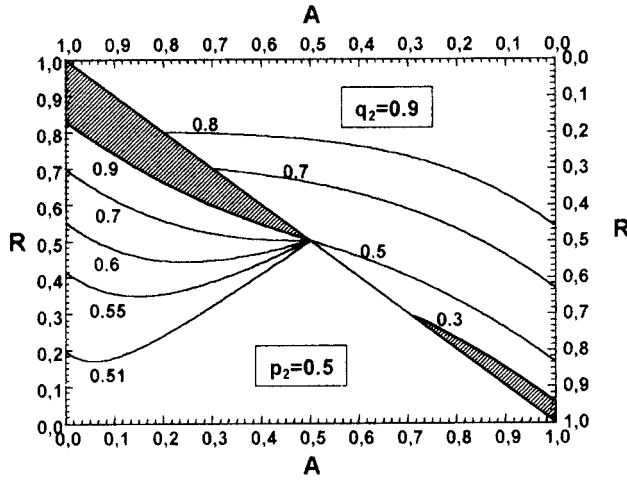
Figure 5. Coaxial-fiber cut-off frequencies for the modes 11, 12, 13 and 21 for different values of  $q_2$  and  $p_2$  in the W2 structure.

Using the equation  $f_3 = 0$  for the structure W2, it is possible to obtain in the plane  $R \times A$  the locus diagram of the regions where the fundamental mode has  $V_3 = 0$  and  $V_3 \neq 0$  for the structure W2. The results are shown in Fig. 6. The shaded regions in this figure indicate where  $V_3 \neq 0$ .

Fig. 5a shows that increasing values of  $p_2$  with constant value of  $q_2$ , increase the values of  $V_3$ . By observing the definition of  $p_2$  and  $q_2$  in Table 3 it can be understood that increasing the value of  $p_2$  keeping  $q_2$  constant, means higher values of  $(n_4 - n_2)$ . This situation implies a smaller confinement of modes. On the other hand,  $q_2$  varies and  $p_2$  is made constant in Fig. 5b. The higher the value of  $q_2$ , the lower the values of  $V_3$ , an effect opposite of increasing  $p_2$  as shown in Fig. 5a. In this case, increasing values of  $q_2$  with  $p_2$  constant means higher values of  $n_3$  and higher modal confinement what reduces the cut-off normalized frequency.

Table 4 - Functions  $f_1$  for each coaxial structure.

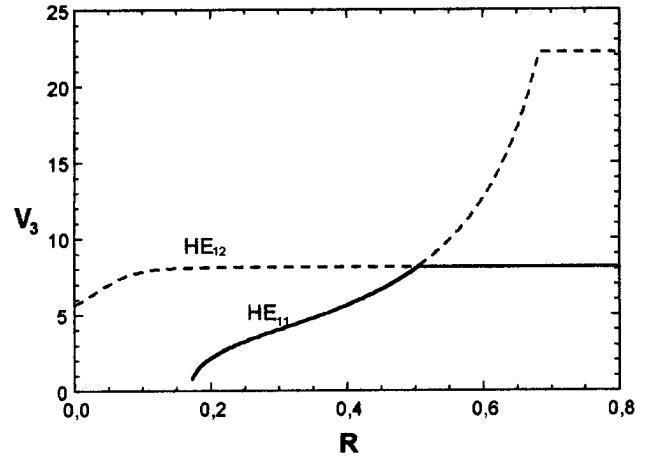
W1	$f_1 = 4 \left[ \frac{(1-(R+A)^2)q_1^2}{1-q_1^2} + \frac{(R+A)^2 p_1^2}{1-q_1^2} + \frac{A^2(1-p_1^2)}{1-q_1^2} \right]$
M1	$f_2 = 4 \left[ (1-(R+A)^2) + p_3^2(R+A)^2 + A^2(q_3^2 - p_3^2) \right]$
W2	$f_3 = -\frac{(R+A)^2 q_2^2}{1-q_2^2} + \frac{A^2}{1-q_2^2} + \frac{q_2^2 - p_2^2}{1-q_2^2}$
M2	$f_4 = -(R+A)^2 + A^2 q_4^2 + 1 - p_4^2$

Figure 6. Delimitation curves between  $V_3 = 0$  and  $V_3 \neq 0$  (shaded) for the fundamental mode of the W2 structure.Table 3 - Definition of  $p$  and  $q$  for the several structures.

$q_1 = \left( \frac{n_3^2 - n_4^2}{n_1^2 - n_4^2} \right)^{1/2}$	$p_1 = \left( \frac{n_2^2 - n_4^2}{n_1^2 - n_4^2} \right)^{1/2}$
$q_2 = \left( \frac{n_3^2 - n_2^2}{n_1^2 - n_2^2} \right)^{1/2}$	$p_2 = \left( \frac{n_4^2 - n_2^2}{n_1^2 - n_2^2} \right)^{1/2}$
$q_3 = \left( \frac{n_1^2 - n_4^2}{n_3^2 - n_4^2} \right)^{1/2}$	$p_3 = \left( \frac{n_2^2 - n_4^2}{n_3^2 - n_4^2} \right)^{1/2}$
$q_4 = \left( \frac{n_1^2 - n_2^2}{n_3^2 - n_2^2} \right)^{1/2}$	$p_4 = \left( \frac{n_4^2 - n_2^2}{n_3^2 - n_2^2} \right)^{1/2}$

When the radius of the nucleus increases, the behavior of  $V_3$  for the modes change substantially, as shows in Fig. 7. This result was obtained for  $A=0.20$ ,  $n_1=1.4658$ ,  $n_2=1.444$ ,  $n_3=1.46$  and  $n_4=1.4587$ . The modes  $HE_{11}$  and  $HE_{12}$  are very close for certain values

of  $R$  with  $V_3$  constant when  $R > 0.5$  for the mode  $HE_{11}$ . For the mode  $HE_{12}$ , two intervals of constant variable  $R$  exist. This behavior is justified when the study of the dispersion curves is made [12]. This study allows to conclude that for certain values of  $R$  the results obtained of the W2 limit structure making  $n_1 = n_2$ , dominates the behavior of the whole structure. In this way, the dispersion curve of the structure W2 always begins in the same value indicating that the cut-off condition doesn't change.

Figure 7. Coaxial-fiber cut-off frequencies of modes 11 and 12 with  $A = 0.20$  and the refractive index cited in the text for the W2 structure.

#### IV.4 M2 structure

The M2 structure presents a behavior similar to that of W2. The same kind of analysis is applicable to this structure and also the fundamental mode has non-vanishing cut-off normalized frequency above a critical value of  $R$ . The expression for the value of  $R$  above which the cut-off conditions of the fundamental mode becomes different from zero can be established imposing the condition  $f_4 = 0$  in Table 4. Then,

$$R = (1 + A^2 q_4^2 + p_4^2)^{1/2} - A \quad (8)$$

A fact that deserves to be mentioned here is the independence of  $V_4$  on  $q_4$ , for small values of  $A$ . Changes in the value of  $q_4$  while keeping  $p_4$  constant does not produce any effect on the values of  $V_4$  because the value of  $A$  is small. Changes in  $q_4$  with  $p_4$  constant means a variation of  $n_1$  according to the definition of these parameters given in Table 3. Therefore, for very narrow rod region, the influence of the refractive index is almost non-existent. This also happens for the M1 structure.

## V Conclusions

This work presents results about the cut-off behavior of four coaxial fibers with four concentric layers. In order to calculate the cut-off normalized frequency numerically, we obtained a transcendental equation for the normalized frequency  $V_i$  ( $i=1,2,3,4$ ) for the four structures. The results show that each pair of structures W1/M1 and W2/M2 have a different behavior. For the structures W1 and M1,  $V_i$  ( $i=1,2$ ) shows an oscillatory characteristic behavior as a function of  $R$  and the fundamental mode always has  $V_i = 0$ . In the case of the structures W2 and M2,  $V_i$  ( $i=3,4$ ) presents a non-vanishing cut-off normalized frequency for the mode  $HE_{11}$ , and there is no oscillatory behavior of the modes. We found expressions for the critical value of  $R$  as function of the parameters of the fiber, starting from which the fundamental mode presents a cut-off different from zero.

## Acknowledgements

The authors acknowledge CNPq Universidade Fed-

eral do Maranhão, for financial support.

## References

- [1] J. R. Cozens and A. C. Boucouvalas, *Electron. Lett.*, **18**, 138 (1982).
- [2] S. Celaschi, J. T. Jesus, D. Dini, A. Juriollo and R. Arradi, *Narrowband All-Fiber Spectral Filters*, CPqD-Telebrás, Campinas-SP.
- [3] F. D. Nunes, C. A. S. Melo and H. F. da Silva, *Applied Optics*, **35**, 388, January (1996).
- [4] F. D. Nunes, H. F. da Silva and S. C. Zilio, *Brazilian Journal of Physics*, **28**, June (1998).
- [5] J. D. Love, W. M. Henry, W. J. Stewart, R. J. Black, S. Lacroix and F. Gauthier, *IEE Proceedings-J*, Vol. **138**, n 5, October (1991).
- [6] Ahmad Safaai-Jazi and Gar Lam Yip, *IEEE Transactions on Microwave Theory and Techniques*, Vol. **MTT-26**, No. 11, 898-903, November (1978).
- [7] M. Abramowitz, *Handbook of Mathematical Functions*, pp. 355-433, Dover Publications (1965).
- [8] A. Safaai-Jazi and G. L. Yip, *Radio Science*, **12**, No. 4, 603-609, July-August (1977).
- [9] Samir F. Mahmoud and A. M. Kharbat, *Journal of Lightwave Technology*, Vol. II, No. 11, 1717-1720, November (1993).
- [10] M. J. Adams, *An introduction to optical waveguides*, pp 272, John Wiley & Sons (1981).
- [11] A. C. Boucouvalas, *Optics Letters*, **10**, No. 2, February (1985).
- [12] H. F. Da Silva, *Doctorate Thesis, IFSC-USP*, August (1999).